Ferry Vessel Propeller Wash Effects on Scour at the Kingston Ferry Terminal (WA, USA)

**Washington State
Department of Transportation**

Office of Research & Library Services

WSDOT Research Report

FERRY VESSEL PROPELLER WASH EFFECTS ON SCOUR AT THE KINGSTON FERRY TERMINAL (WA, USA)

Sam Kastner[1], Chris Stearns[2], Alex Horner-Devine[1], and Jim Thomson[1,3]

[1]Civil & Environmental Engineering, University of Washington, Seattle, WA, USA

[2]Terminal Engineering, Washington State Ferries, Seattle, WA, USA

[3]Applied Physics Lab, University of Washington, Seattle, WA, USA

Prepared for

The State of Washington

Department of Transportation

Roger Millar, Secretary

October 31, 2019

TECHNICAL REPORT DOCUMENTATION PAGE

1. Report No. WA-RD 899.1	2. Government Accession No.	3. Recipient's Catalog No.
4. Title and Subtitle Ferry vessel propeller wash effects on scour at the Kingston ferry terminal (WA, USA)		**5. Report Date** October 31, 2019
		6. Performing Organization Code
7. Author(s) Samuel E. Kastner, Chris Stearns, Alex R. Horner-Devine, Jim M. Thomson		**8. Performing Organization Report No.**
9. Performing Organization Name and Address University of Washington Department of Civil & Environmental Engineering More Hall Seattle, WA, 98195		**10. Work Unit No.**
		11. Contract or Grant No. WSDOT Grant T1461, Task Order 55
12. Sponsoring Agency Name and Address Washington State Department of Transportation		**13. Type of Report and Period Covered** Final Report (February 2018-October 2019)
		14. Sponsoring Agency Code WSDOT
15. Supplementary Notes		

16. Abstract

We investigated the hydrodynamic causes of severe erosion at the Washington State Ferries ferry terminal in Kingston, WA, where a cliff-like bathymetric feature has shifted shoreward in recent years, forcing repairs on the slip's bridge pilings. High resolution measurements of velocity and estimates of turbulent bed stress were made during vessel arrivals and departures during two deployment periods in March and April 2018. Calculated bed stresses (and maximum velocities) were found to be 10-100 (30-50) times larger during vessel arrivals and departures than background levels. The structure of the wash is modified by the bathymetry such that steeper bathymetry leads to more reflection of the propeller wash. Bed stresses were higher during vessel departures than arrivals, corresponding to higher vessel acceleration during departures. Additionally, during departures, lower tidal stages correspond to higher bed stresses, because the propellers are closer to the seabed. During arrivals, larger vessels generated higher bed stresses. In this work, we develop, assess, and use an empirical model for bed stress that takes into account these dependencies. Using this model, we determine that the most important factor for cumulative vessel stress is the frequency of use of a given slip. Additionally, shallower ground lines will be exposed to higher bed stress than deeper ground lines, so modifications to the existing bathymetry should take into account both the effect of shallower depth and milder slope.

17. Key Words Hydrodynamics, Wakes, Turbulence, Scour, Ferry terminals, Vessel operations	18. Distribution Statement		
19. Security Classif. (of this report) Unclassified	**20. Security Classif. (of this page)** Unclassified	**21. No. of Pages** 51	**22. Price**

Form DOT F 1700.7 (8-72) Reproduction of completed page authorized

Disclaimer

The contents of this report reflect the views of the author(s), who is (are) responsible for the facts and the accuracy of the data presented herein. The contents do not necessarily reflect the official views or policies of the Washington State Department of Transportation, Federal Highway Administration, or U.S. Department of Transportation [and/or another agency]. This report does not constitute a standard,

Table of Contents

Figures

Tables

EXECUTIVE SUMMARY

Objectives

In recent years, severe scour at the Kingston ferry terminal has caused concern for terminal safety, as an undersea cliff face at Slip 1 has migrated shoreward and through the bridge seat towards the onshore trestle structure. In this work we examine the influence of vessel propeller wash on erosion by characterizing the vessel wake and wash structure, and developing a predictive model of seabed stress, the dynamical quantity that leads to erosion.

Observations

We used state-of-the-art oceanographic instruments to measure velocity and turbulent bottom stress at the seabed and along the length of each of the two slips at the Kingston ferry terminal during vessel arrivals and departures. We develop an empirical model for bed stress based on the the observed turbulent stresses and apply it to a 9 year long long record of vessel activity and tidal stage.

Results

Vessel arrivals and departures are associated with $10 - 30\times$ larger velocities and $10 - 100\times$ larger stresses than ambient conditions. The wake and wash structure is affected by the differences in bathymetry between Slip 1 and Slip 2, particularly the steeper slope at Slip 1. Different variables influence the magnitude of bed stresses on arrivals and

departures. During departures, higher bed stresses occur at lower depths (due to tidal variability), while on arrivals, higher bed stresses are primarily associated with larger vessels arriving at the terminal.

Conclusions

Our model shows that over time periods longer than one to two weeks, the most important driver of cumulative seabed stress is the frequency of vessel activity. The stress on the seabed during departures can be influenced by changing the seabed elevation, and we show that filling the scour hole at Slip 1 is likely to cause an increase in seabed stress. This must be taken into account when choosing a sediment grain size to use for fill.

INTRODUCTION

The Kingston ferry terminal, in Kingston, WA (USA), has experienced rapid erosion in recent years. A steep drop at one of the slips has shifted shoreward, leading to erosion mitigation efforts. This work investigates the role of ferry-generated turbulence in causing this erosion. Specifically, we determine the magnitude of the bed stresses caused by ferry arrivals and departures compared to quiescent periods, and the dependencies of this ferry-induced bed stress on tidal, climatological and vessel properties.

The objective of our work is to characterize the ferry propeller wash in order to develop a model to better predict scour at ferry terminals. We accomplish this using high resolution measurements of turbulence at the seabed at both slips of the Kingston ferry terminal, leveraging dependencies on seabed depth, and vessel characteristics to simplify the model. We then apply the model to a 9-year time series of vessel activity and tidal stage data, as well as various along-slip profiles of seabed elevation.

Scour, or erosion near a submerged structure, is a problem inherent to marine infrastructure [Chin et al., 1996, Hamill et al., 1998, Yuksel et al., 2012, Tan and Yuksel, 2018]. Scour occurs when turbulence near the seabed is enhanced around submerged structures, leading to local erosion. In the case of a bridge pile, this normally leads to a scour hole around the pile, compromising the embedment of the pile [Tan and Yuksel, 2018]. Scour due to propeller wash has been found to be a function of the wash velocity, the sediment grain size, the propeller size, and the distance of the propeller above the seabed [Tan and Yuksel, 2018].

Large vessels such as ferries create both a wake and a propeller wash, two hydrody-

1

Figure 1. Experimental setup and erosion time series

(a)

Terminal Building
Towers
Wingwalls
Trestle
Bridge Seat
Transfer Span
Apron
Dolphin

🟠 Acoustic Doppler Current Profiler (ADCP)

🟢 Acoustic Doppler Velocimeter (ADV)

(b)

Slip 1
Slip 2

(c) **Bridge Seat Erosion**
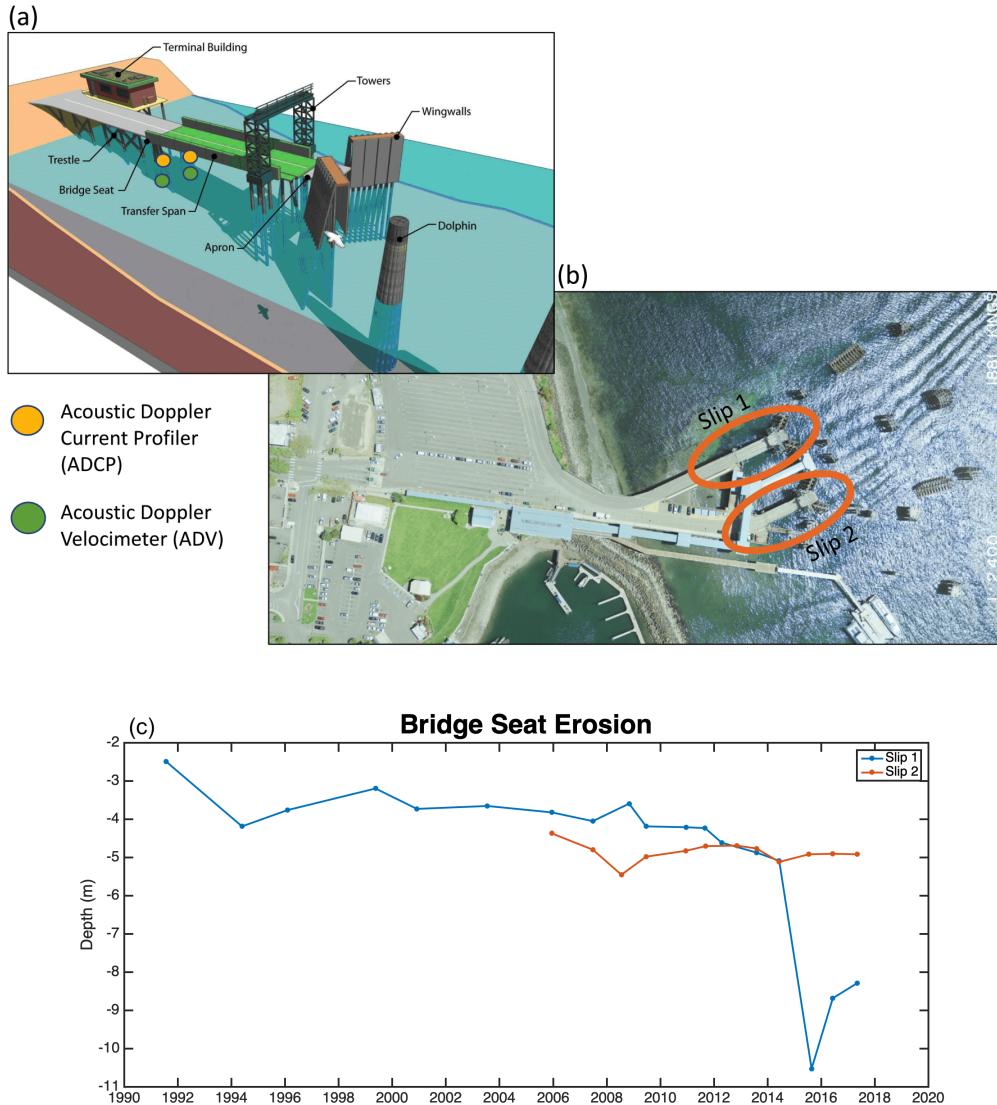
Figure 1: Experimental setup & bed elevation time series at Kingston ferry terminal, WA. (a) shows the instruments as deployed at both slips, with yellow dots corresponding to Acoustic Doppler Current Profilers at mid-depth on both bridge seat pilings, and green dots corresponding to Acoustic Doppler Velocimeters at the bottom of the same pilings; (b) shows the relative positions of Slip 1 and Slip 2 (circled in orange); (c) shows time series of erosion near the bridge seat of Slip 1 (blue) and Slip 2 (red).

namic features that may contribute to scour at a ferry terminal. The vessel wake is a wave that radiates away from the vessel, while the propeller wash is turbulence generated by the vessel's propeller [Chin et al., 1996]. As a wave, the vessel wake is a smoother feature than the wash's inherently turbulent nature. The passage of a vessel involves both of these processes, and both can lead to scour [Chin et al., 1996, Hong et al., 2013].

RESEARCH APPROACH & PROCEDURES

Observational methods

Measurements were made at the Washington State Ferries, Kingston Ferry Terminal on the Puget Sound (Figure 1). The Kingston terminal has two slips. Slip 1, to the north, receives the most vessel traffic and has developed a sharp cliff face directly underneath its bridge seat (Figure 1c). The sharp cliff face has eroded further shoreward on the south side of the slip than on the north side of the slip. Slip 2, to the south, has a gentler, more consistent seabed slope, and receives less vessel traffic (Figure 1c). The Kingston terminal seabed consists of mixed sediment types, with larger cobbles mixed in among finer sediment.

Instrumentation packages were deployed at Slip 1 from March 15-28, 2018, and at Slip 2 from April 25-May 15, 2018 (Table 1) . These instrumentation packages included two NorTek Vector Acoustic Doppler Velocimeters (ADVs) mounted to the base of the north and south bridge seat piles, and two NorTek Signature 1000 Acoustic Doppler 2nd generation Current Profilers (AD2CPs) mounted to the north and south bridge seat piles facing the offshore end of the slip (Figure 1). The ADVs measure velocity at a single point close to the seabed at a frequency of 16 Hz. The AD2CPs measure velocity along five 20 m long acoustic beams with measurement bins every half meter, and sampling frequency of 8 Hz. One central acoustic beam is pointed in the along slip direction, with four other beams directed 25° to left, right, up and down of center.

The deployment depth of each instrument varies slightly from slip to slip and piling to piling. The instruments collected data in 512 second bursts followed by 208 seconds of no collection, for a total cycle time of 12 minutes. During the period of time when a

slip was instrumented, ferry traffic was redirected to that slip when possible. The analysis presented in this paper focused on the ADV data.

Dates	Location		Sensor Depths (m)	
	Slip	Piling	AD2CP	ADV
March 15-28, 2018	1	North	5.6	9.8
March 15-28, 2018	1	South	5	5.9
April 25-May 15, 2018	2	North	3.7	4.2
April 25-May 15, 2018	2	South	4.4	5.1

Table 1: Instrument deployment periods, locations, and depths.

Two different classes of Washington State Ferries vessels, the Jumbo and the Jumbo Mark II, were operated on the Edmonds-Kingston route during instrument deployment. The Jumbo class vessels *M/V Spokane* & *M/V Walla Walla* have displacements of approximately 4860 long tons each, and the Jumbo Mark II class vessel *M/V Puyallup* has a displacement of 6184 long tons. The vessels are double-ended, with symmetric propulsion systems and boarding ramps on each end, allowing the vessels to arrive and depart at the terminal without changing orientation. Propeller wash is directed along the slip, as the

slip-facing propeller is active for braking on arrivals and propulsion on departures.

In order to calculate the turbulent stress exerted on the bed during vessel arrivals or departures, we use Reynolds' decomposition to split the axial, cross-bridge and vertical velocity components measured by the near-bed ADVs into a mean flow and a perturbation such that

$$u_i = \overline{u_i} + u'_i \tag{1}$$

where u_i is the total value of a velocity component in one of three orthogonal directions, $\overline{u_i}$ is the mean flow, and u'_i is the perturbation velocity. $\overline{u_i}$ is taken to be the low-pass filtered velocity used in smoothing the profile to detect events, and thus u'_i may be calculated such that $u'_i = u_i - \overline{u_i}$.

Wash detection

Vessel wash periods are identified in the measurement record based on observed velocity peaks. A threshold in velocity of 50 cm/s was applied to the ADV data to determine when a vessel arrives or departs the terminal. If, during a data collection burst, the velocity exceeds this threshold after the application of a moving median filter with a 2 second window, this burst is marked as a vessel arrival or departure. An example of a data collection burst is shown in Figure 2. Overall, implementing the 50 cm/s threshold on data after using a low-pass filter results in the lowest number of false positives, i.e. instances of ambient conditions incorrectly labelled as arrival or departure events.

Each detected event lasts 1-3 minutes, after which the vessel-induced velocity signature has diminished completely and quiescent conditions return (Figure 2). Partial events

may be observed when the instruments resume their data collection period after the beginning of the arrival or departure, or if the instrument stops sampling before the end of the arrival or departure. As the initial burst of velocity is the strongest, a partial wake at the end of the data collection period could be labelled as an arrival or departure. A partial wake at the start of data collection is more likely not to be labelled an arrival or departure, as the initial burst of strong velocity occurs before the instruments have resumed data collection. Additionally, an exceedance of the threshold velocity observed by the ADV on one piling, but not the other, was marked as a vessel arrival or departure for both ADVs.

Figure 2: Example vessel arrival time series
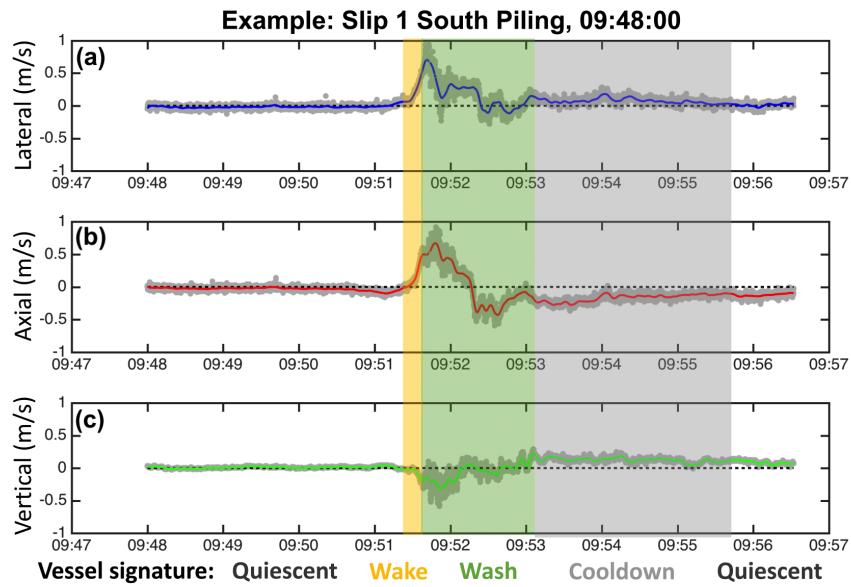
Figure 2: Example vessel arrival velocity time series (10 minutes total) from an entire data collection burst at the south piling of Slip 1. All periods are labelled. Both quiescent periods are shaded white, the wake period is shaded gold, the wash period is shaded green, and the cooldown period is shaded grey. Panel (a) shows the lateral velocity, (b) shows the axial velocity, and (c) shows the vertical velocity. Solid colored lines indicate mean velocity, while the grey shaded areas indicate the perturbations around this mean.

Turbulent stress calculations

The Reynolds stress, τ, is the stress that is generated by turbulent fluctuating velocities,

$$\tau = \rho \overline{u'_i u'_j} \tag{2}$$

where ρ is the density of the water. This formulation results from applying Reynolds' decomposition to the Navier-Stokes equations, and assumes the turbulence is isotropic and the flow is steady.

We calculate a mean Reynolds stress over the 30 seconds before and 120 seconds after the peak of the mean velocity time series during a burst, regardless of whether the mean velocity crosses the event threshold. This allows for the inclusion of the an entire arrival or departure in the calculation, and forces the number of data points in fully captured arrivals or departures and quiescent periods to be the same. Partially captured events have fewer data points, as the record will not extend for the full 30 or 120 seconds in backward or forward in time from the peak velocity.

OBSERVATIONAL PERIODS

Each deployment lasted for an entire spring-neap tidal cycle, during which wind speeds varied between 0-15 m/s, with events of over 10 m/s lasting approximately 36 hours (Figure 3). Bed stress varies between 10^{-2} and 10^2 Pa (Figure 3). This variability is primarily driven by vessel arrivals and departures, which are associated with bed stresses on average 100 times larger than quiescent conditions. The prolonged wind event at the end of the deployment period on Slip 1 is associated with a slight rise in the quiescent bed stress, but does not appear to have a strong influence on the bed stress associated with arrivals and departures. Based on this observation we conclude that adjustments made by vessel operators during strong wind conditions do not significantly influence the bed stress upon arrival or departure.

Figure 3: Climatological conditions and bed stress
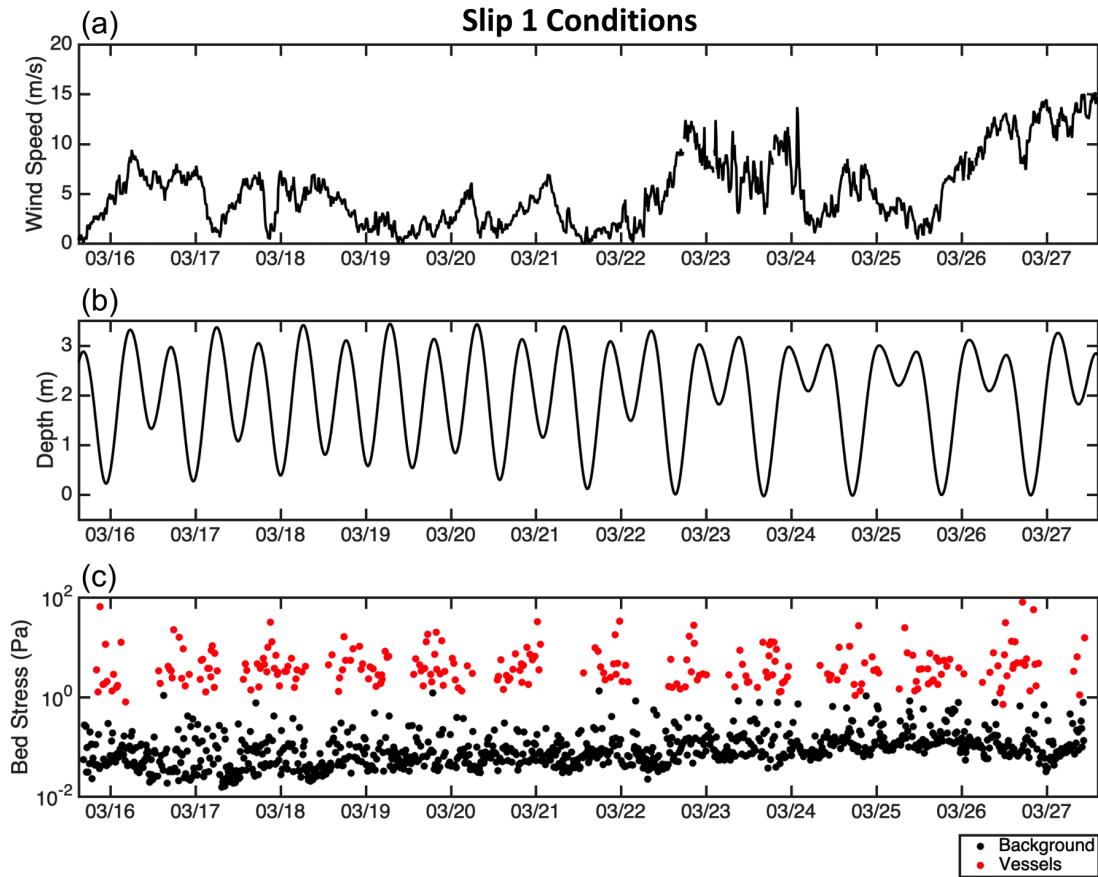
Figure 3: Climatological conditions time series during the deployment at Slip 1. Panel (a) shows wind speed; (b) shows tidal depth; (c) shows bed stress, with red points corresponding to vessel arrivals and departures and black points corresponding to bursts with no vessel activity.

WASH CHARACTERIZATION

Seabed velocity structure

A typical arrival or departure event has four distinct phases (Figure 2). The first and last are quiescent periods, in which background low flow conditions dominate. The second is the large mean velocity spike associated with the wake of the vessel (lasting approximately 10-20 seconds). The wake phase is highly coherent, with minimal turbulent fluctuations (lasting 30-60 seconds). The third phase is associated with the propeller wash of the vessel; the mean velocity is smaller and turbulent fluctuations are large (lasting approximately 1 minute). The last phase is a cool down period, over which time both the mean velocity and the turbulent fluctuations decay to quiescent levels. The largest mean velocities occur in the along-slip component, followed by the cross-slip component, and then the vertical component.

In general, a higher value of maximum velocity during a data collection burst corresponds to a higher bed stress (Figure 4). This is true for arrivals, departures, and quiescent periods. It is known that the propeller wash is the dominant source of turbulence close to a vessel, consistent with our result that the propeller wash contains larger fluctuations than the wake [Chin et al., 1996]. However, the positive correlation between the maximum velocity and the bed stress observed during a data collection burst implies that the speed of the wake and the turbulent intensity of the wash are linked. Thus, the initial velocity spike due to the wake of an arrival or departure does not directly cause high bed stress, but is instead associated with a larger bed stress due to the subsequent propeller wash.

Maximum velocity for all vessel arrival and departures are shown as a histogram
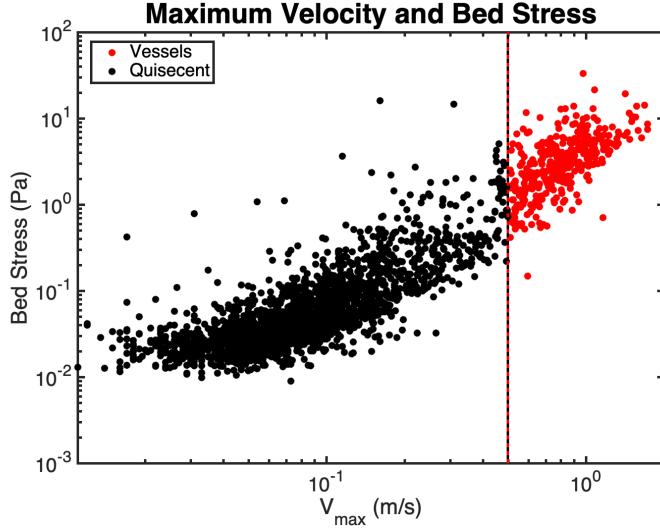
Figure 4: Maximum filtered velocity and bed stress at the south piling of Slip 1 for full vessel arrivals and departures (red), partial arrivals and departures below the maximum velocity threshold (grey) and quiescent periods (black). The dotted black and red line indicates the 50 cm/s threshold for arrival and departure identification.

for each slip and piling in Figure 5, and the mean and standard deviation of maximum velocity are shown for each slip and piling in Table 2. Slip 1 experiences lower maximum velocities, which is consistent with the greater depth of the ADVs and the seabed at Slip 1 than Slip 2. In general, maximum velocities do not exceed 1.75 m/s, but are 0.82 m/s on average for the shallower depths of Slip 2, where one standard deviation accounts for variability of 0.31 m/s, with daily occurrences of velocities close to 1.5 m/s (Table 2). Note that the distributions are skewed right. At Slip 1, maximum velocities are on average 0.49 m/s, with daily occurrences of velocities close to 1 m/s. The standard deviation at slip 1 varies by a factor of two from the north to south piling.

13

Figure 5: Maximum velocity histograms
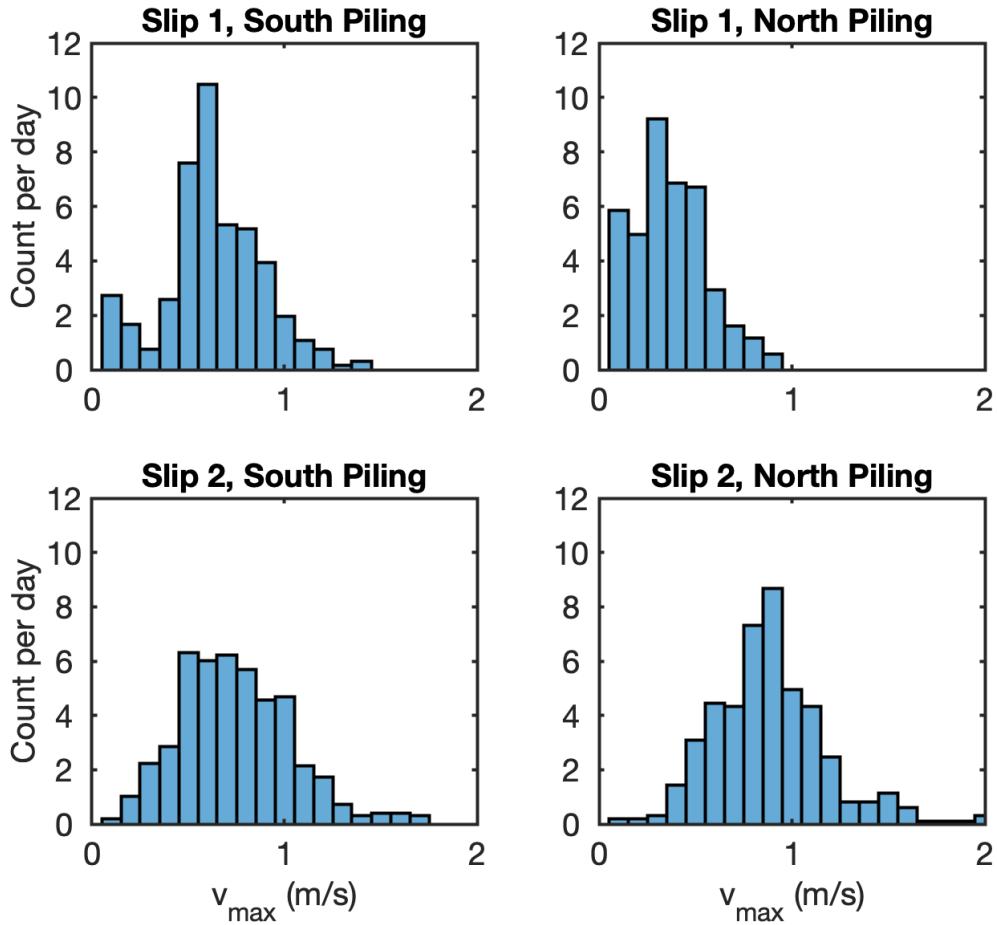
Figure 5: Histograms of maximum velocity during vessel arrivals and departures for each slip and piling. The histograms are normalized such that the y-axis indicates the daily frequency of each 0.1 m/s velocity bin.

Location		Max Velocity (m/s)		
Slip	Piling	Mean	St. Dev.	ADV Depth (m)
1	North	0.323	0.213	9.8
1	South	0.655	0.416	5.9
2	North	0.890	0.311	4.2
2	South	0.752	0.325	5.1

Table 2: Mean and standard deviation of maximum velocity at both slips for both pilings, and sensor deployment depths relative to mean lower low water.

We observe that maximum velocity at Slip 1 is lower than at Slip 2, which is consistent with the depth at Slip 2 being shallower than Slip 1, resulting in the propeller being closer to the bed. However, binning the maximum velocity observed during each vessel arrival and departure in depth does not reveal a large trend within each site (Figure 6). In this calculation, the depth variability comes from the tidal range, as the ADV is at a greater depth at high water than low water. While it is likely that the relatively greater depth at Slip 1 leads to lower maximum velocities at the seabed, this effect is difficult to differentiate from the impact of bathymetry differences at each site. There does appear to be a small decrease of maximum velocity in depth at the south piling of each slip. The distributions of maximum velocity for the south pilings are also more similar than those for the north pilings, although the distribution for Slip 2 does not have as large a peak as the Slip 1

distribution (Figure 6).

The example wake shown in Figure 2 shows periods of onshore (positive) and off-shore (negative) velocity in the axial structure. These different flow directions could affect sediment transport processes in different ways, as offshore flow is directed downslope with respect to the seabed. Offshore flow could thus be more effective at transporting resus-pended sediment from the seabed than onshore flow, as gravity and the current direction are co-aligned. The relative magnitude of the maximum offshore and onshore velocity for vessel arrivals and departures differs between the slips (Figure 7). At Slip 2, where the seabed slope is gentler, the maximum onshore velocity is larger than the maximum offshore velocity, indicating that the wake and wash is mostly dissipated as it propagates onshore. At Slip 1, however, the maximum onshore and offshore velocities are the same, indicating a significant reflection of the wake and wash. This is likely due to the seabed cliff face at Slip 1, which is expected to locally reflect the wake and wash. A similar process occurs when surface gravity waves break nearshore. Beaches with milder slopes reflect less wave energy and are referred to as "dissipative" beaches, while beaches with steeper slopes re-flect more wave energy and are referred to as "reflective" beaches [Wright et al., 1979]. This more reflective nature of the steeper Slip 1 bathymetry and the more dissipative nature of the milder Slip 2 bathymetry fit this framework, showing the importance of bathymetry in the wake and wash hydrodynamics.

Figure 6: Profiles of maximum velocity in depth
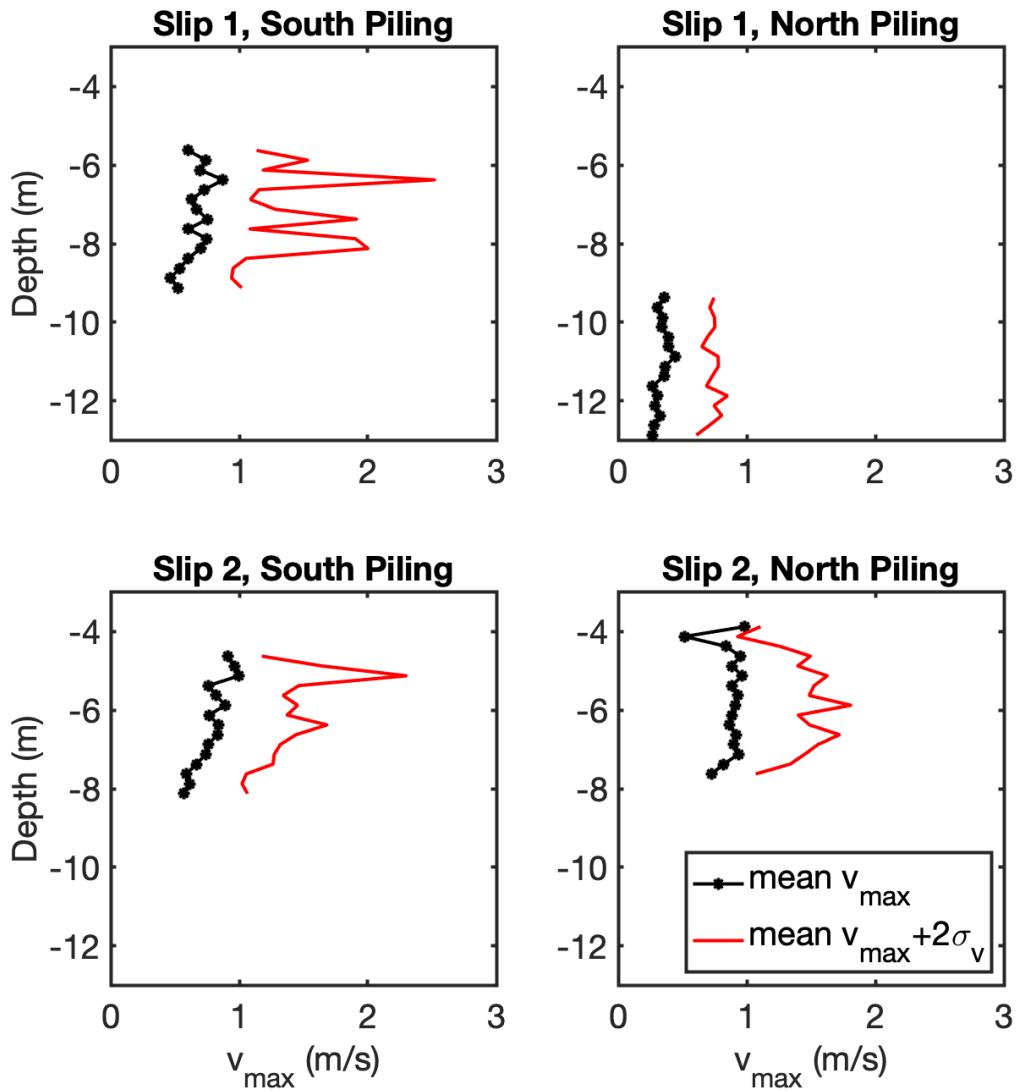
Figure 6: Profiles of the mean maximum velocity in 0.25 m steps of tidally varying depth bins at each slip and piling are shown in black. An upper limit for maximum velocity is given by the red line, which shows the velocity two standard deviations above the mean for a given bin.

Figure 7: Onshore and offshore velocity comparison
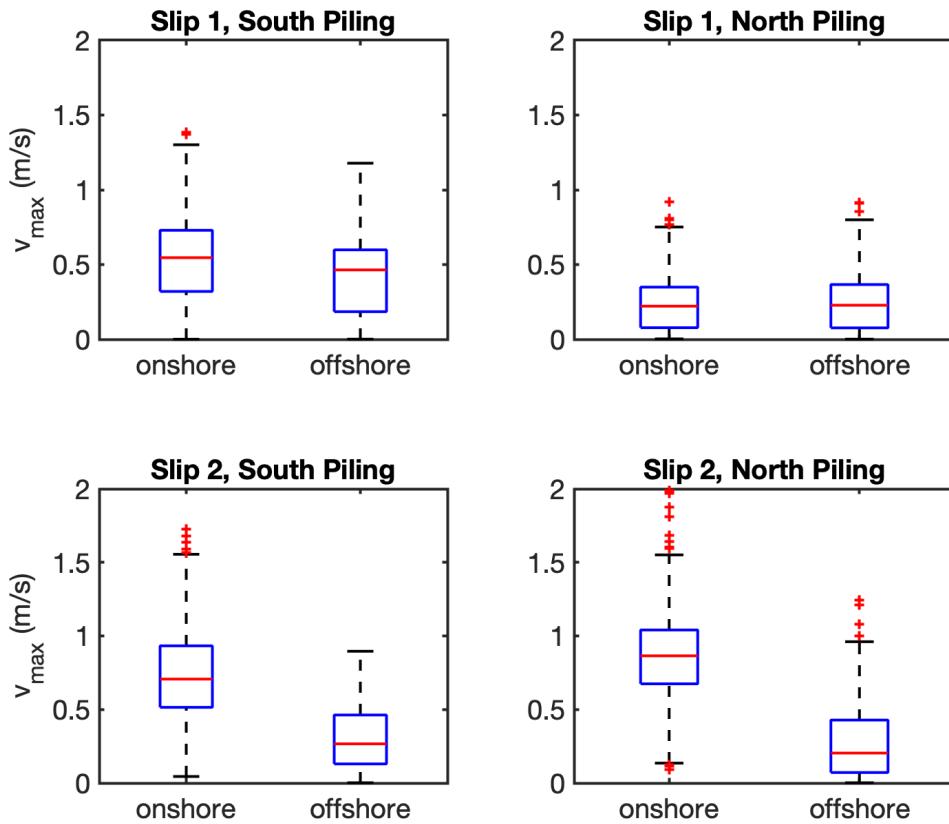
Figure 7: Box plots of onshore and offshore maximum velocity for all vessel arrivals and departures at each slip and piling. The red line in the middle of each box shows the median, while the interquartile range is shown by the box edges. The whiskers indicate an extreme value, and red crosses above the whiskers indicate outliers. Outliers are determined by the Matlab *boxplot* function. Note that infrequent velocities above 2 m/s have not been shown.

Along-slip velocity structure

Analysis of the laterally profiling AD2CP data yields some insight into the along-slip velocity structure. The AD2CPs were oriented so that their center beam was directed along-slip (toward the vessel), and therefore measures along-slip velocity. By applying the same vessel detection algorithm from the ADV data to the AD2CP dat, we obtain a measure of maximum velocity in each AD2CP bin for every vessel arrival and departure. Figure 8 shows the along-slip structure of this maximum velocity, which averages over all depth variability due to the tide.

It is important to note that the structure of the measured along-slip velocity component is not necessarily indicative of the principal wash velocity structure due to the contributions of cross-slip and vertical velocities. This is especially true far from the AD2CP, where the wash is narrower and potentially constrained by the terminal's wing walls. The complications due to the wash and beam geometry are visible as a decrease in velocity far from the AD2CP at the north piling of Slip 1 in Figure 8.

Overall, the variability due to the along-slip structure is not large compared to the magnitude of the mean maximum velocity or the variability of the mean maximum velocity at each along-slip position. If we assume that maximum velocity and bottom stress have a similar spatial variation in the along-slip direction, the model developed in section can be applied at any along-slip distance to assess the bottom stress.

Figure 8: Along-slip maximum velocity profiles
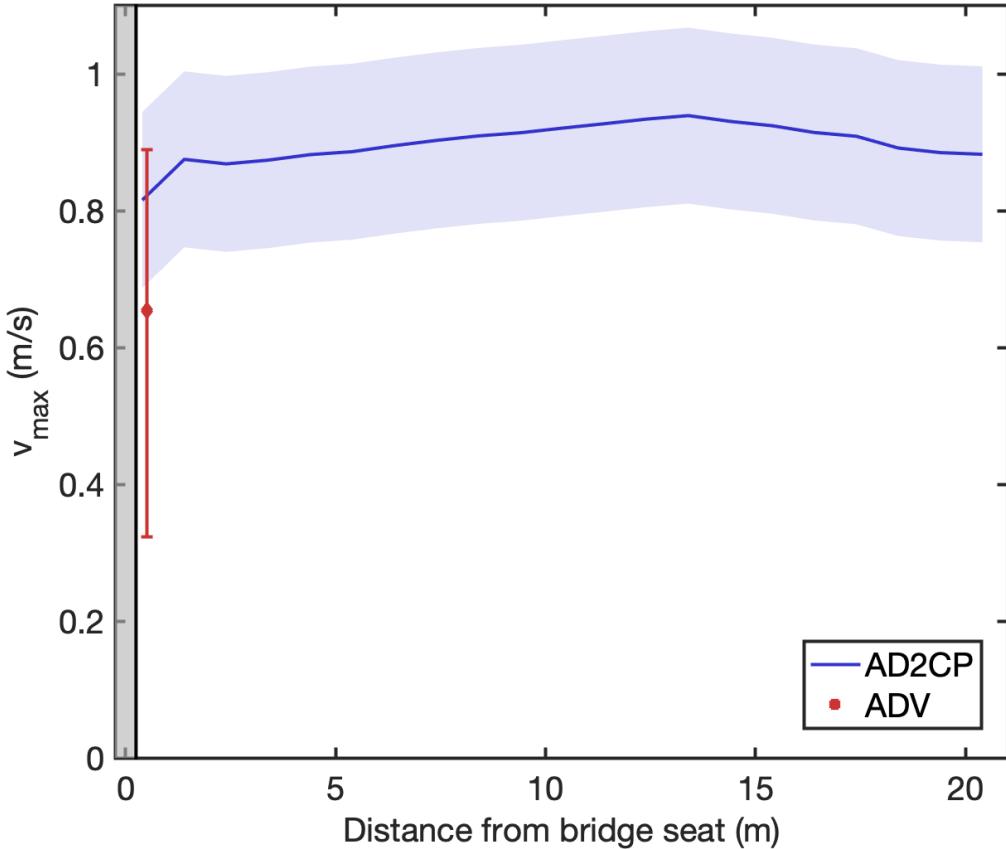
Figure 8: Along-slip profile of the mean maximum velocity, taken as the average over all slips, pilings, and tidal depths. The bridge seat is located on the left, while the ferry arrives on the right. The shaded gray area indicates the approximate location of the pilings. The blue line indicates the AD2CP profile, with the shaded error bar indicating the approximate variability between slips and pilings. The red point indicates the mean maximum velocity for all ADV data, with the error bar indicating the approximate variability between all slips and pilings.

BED STRESS: DEPENDENCIES & IMPLICATIONS

The bed stresses during vessel arrivals and departures vary in magnitude from approximately 1 to 100 Pa. Comparison of the wind and tidal records with the measured stresses (Figure 3) indicated that the variability in the stress is not explained by wind or tidal forcing. No significant correlations were found in a statistical comparison between wind, tides and stresses, confirming this result (not shown). We find that the difference in the bed stress associated with vessel arrivals and departures is the main driver of bed stress variability. Vessel arrivals are generally associated with lower bed stresses than vessel departures (Table 3) at the south pilings of both slips, with similar stresses at the north pilings. The difference at the south pilings could be due to deceleration during arrivals being smaller than acceleration during departures and directionality of the propeller wash. This is discussed in section .

Location		Mean Stresses (Pa)			
Slip	Piling	All	Arrivals	Departures	ADV Depth (m)
1	North	2.4	2.5	2.3	9.8
1	South	4.5	4.0	5.0	5.9
2	North	3.6	3.7	3.5	4.2
2	South	3.4	3.0	3.7	5.1

Table 3: Mean stresses at both slips for both pilings, and sensor deployment depths relative to mean lower low water.

Depth dependence

Vessel arrivals and departures occur at varying water levels as depth at the ferry terminal oscillates due to the tide,. Intuition would suggest that at lower water levels bed stress would be higher because the propeller is closer to the seabed. Indeed, vessel departures are associated with a strong relationship between bed stress and depth (Figure 9). Bed stress data were bin averaged by depth before fitting, disregarding depth bins with a low number of measurements. During vessel departures, tidal elevation is the primary source of variability in the observed bed stress; higher bed stresses occur at lower water levels (Figure 9). There is no observable relationship between bed stress and depth for vessel arrivals at either piling of either slip (not shown). It is possible that the high acceleration during departures advects the propeller wash to the seabed. During arrivals, however, the lower

22

deceleration results in a more diffusive process which results in the turbulence decaying to a consistent level before it reaches the seabed.
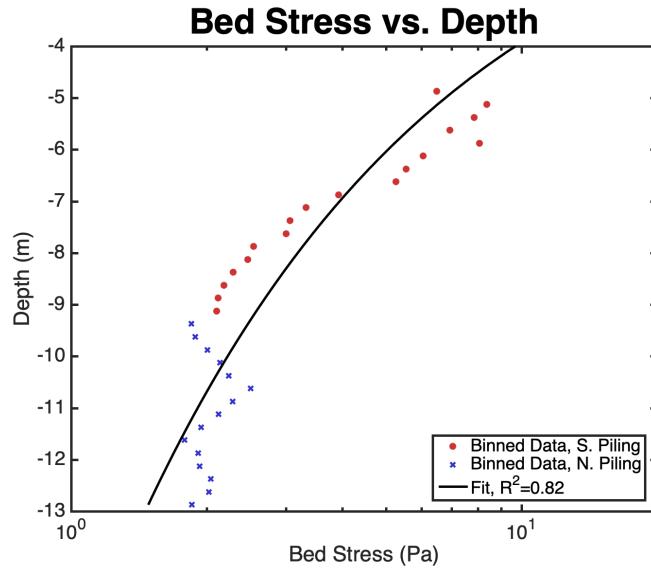
Bed Stress vs. Depth

Figure 9: Profiles of bed stress at varying depths for departures at Slip 1. The binned data is shown as colored points (red crosses for the north piling, blue circles for the south) and the fit is shown as a solid black line with an R^2 value given in the legend.

Vessel dependence

Two different-sized classes of vessels operated during the measurement period; the Jumbo Mark II class *M/V Puyallup* has 50% higher displacement than the Jumbo class *M/Vs Walla Walla* and *Spokane*. As more thrust is necessary to change the speed of a larger vessel, it would follow that the acceleration and deceleration behaviors of different vessel

types are different. The disparity in vessel size results in higher bed stress during *Puyallup* arrivals than *Spokane* or *Walla Walla* arrivals (Figure 10). This relationship between displacement and bed stress is not observed during vessel departures (not shown). Different acceleration and deceleration behaviors between arrivals and departures for different vessel classes could account for the lack of relationship between vessel size and bed stress upon vessel departure. It is important to note that the *M/V Puyallup* was used 80% less frequently than the *M/V Spokane* and *M/V Walla Walla* during the study period.
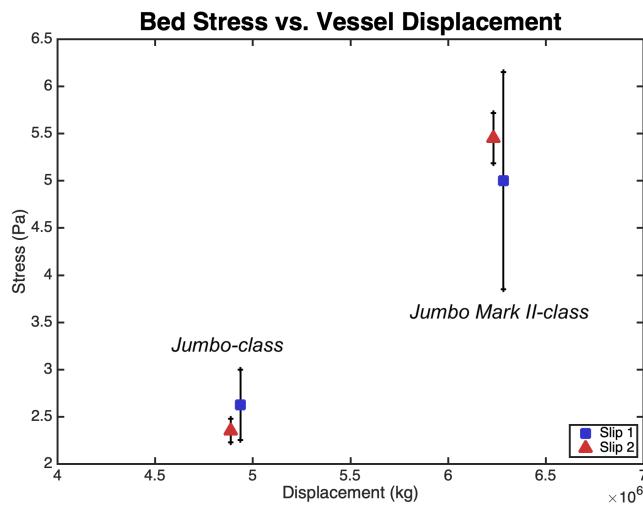
Figure 10: Bed stress by vessel displacement, averaged over both pilings at each slip. Slip 1 values are shown by blue squares, Slip 2 values by red triangles. Whiskers show standard error bounds. Each vessel in a vessel class has the same displacement. The apparent small difference in displacement between slips is for legibility only and does not reflect actual differences in vessel displacement.

Sediment transport

While the measurements do not include direct estimates of scour, it is worth considering how the observed stress magnitudes are expected to influence the bed. We start by considering initiation of motion, based here on thresholds described, for example, in Shields [1936] and Julien [2010]. Initiation of sediment motion is a necessary condition for scour and thus constitutes a minimum threshold for the stress that can cause scour. The mean stress observed during vessel arrivals and departures is 3.5 Pa, large enough to move fine to medium gravel ($\sim$ 8 mm diameter). The largest bed stresses observed are greater than 40 Pa, large enough to move very coarse gravel ($\sim$ 5 cm diameter). The bed stresses during events vary between 1 and 100 Pa, while the stresses during quiescent periods are mostly lower than 0.5 Pa, moving very coarse sand ($\sim$ 1 mm diameter) at maximum. The mean quiescent bed stress is 0.2 Pa, corresponding to the threshold stress for medium sand ($\sim$ 0.25 mm diameter). This relationship between bed stress and particle size assumes a horizontal seabed, and so it is likely that larger particles will be more easily mobilized given the slope of the seabed, particularly for the cliff face at Slip 1. Thus, the large mean bed stresses during departures and arrivals are almost certainly strong enough to initiate motion among the small particles at the seabed, and the maximum stresses are large enough to initiate motion among the large cobbles embedded within the smaller particles. This could lead to two modes of erosion: the gradual erosion of smaller particles around an embedded larger cobble by average vessel-induced stresses until the cobble is able to fall away from the rest of the seabed, or the direct removal of cobbles by vessel-induced stresses close to the maximum observed.

Previous laboratory experiments on scour due to propeller washes have found that scour depends on many parameters, including the depth of the propeller, the distance between the propeller and the seabed, the grain size of the sediment at the seabed and the velocity of the propeller wash [Hong et al., 2013, Tan and Yuksel, 2018, Yuksel et al., 2018]. Based on our analysis, we observe dependence on similar quantities: the water depth and the size of the vessel, which are analogous to the seabed-propeller distance and the initial velocity of the propeller wash, respectively. However, our analysis uses direct calculations of bed stress as opposed to the properties of the propeller wash jet used in the experimental studies of Yuksel et al. [2018].

Inter-piling and inter-slip variability

Bed stress varies both between the pilings on a particular slip for a given arrival or departure, and between slips. In particular, stresses are slightly higher at Slip 1 than Slip 2 (see Table 3). The average wash stresses at Slip 1 and Slip 2 are 4.8 and 3.8, respectively. This is opposite from expected trends, as the seabed (where the ADVs were located) is deeper at Slip 1 than at Slip 2, and thus father from the propeller. A different mechanism is necessary to explain the advection of propeller wash turbulence to the seabed at Slip 1 than at Slip 2. Since the two slips have different bathymetry, with Slip 1 having a shear cliff face and Slip 2 a gentle slope, we posit that the turbulence either self-advects down or reflects off the cliff face. Such a process could result in more intense turbulence at the seabed at Slip 1, leading in turn to higher bed stresses. This is consistent with the observed differences in the backwash velocity (section), which indicated that there was more reflection of the

propeller wash at Slip 1 than Slip 2.

The bed stresses during vessel arrivals and departures at the south pilings of both slips are higher than at the north pilings (Table 3). This likely indicates that there is a southern preference in the direction of the propeller wash, as the higher stresses indicate that turbulence is more energetic at the south piling, and thus has not had as much time to diffuse. The lack of clarity in a signal between arrivals and departures at the north pilings support the conceptual picture of the propeller wash being directed at the south piling before diffusing to the north, as this could result in similar signals at the north piling due to diffusion of turbulence. A southerly directed wash would help explain the spatial pattern of erosion in the cliff face at Slip 1, as this directionality would cause stronger seabed erosion at the southern piling. The rotational direction of the vessels' propellers might drive the propeller wash toward the south, resulting in these higher bed stresses. It is important to note that the large difference between the stresses at the south and north pilings at Slip 1 must be partially due to the large difference in water depth at those pilings, which resulted in the north piling ADV being 3.9 m deeper than the south piling ADV (Table 3).

MODEL DEVELOPMENT & VALIDATION

The overall objective of this work is to develop a predictive understanding for the scour due to ferry propeller wash. Our turbulence data show that the measured stress depends strongly on the water depth and also on the lateral location of the measurement. This is consistent with a conceptual picture of the prop wash as a turbulent jet extending back from the vessel to the pilings, whose intensity decreases vertically and horizontally away from the main axis of the jet. Engineering jets are often modeled with a Gaussian structure that accounts for this shape. In order to generate a predictor for the scour potential due to bed stress from the prop wash, we fit our bed stress measurements to a Gaussian model. We choose vessel departures because departures are associated with higher stresses and show stronger spatial dependence. We are unable to fit the near-surface velocity structure due to our sensor depths. We assume the turbulent wash exhibits a Gaussian profile in depth and across-slip distance, as is common for turbulent jets. The wash can then be modeled by the equation

$$\tau = \alpha e^{-\left(\frac{y-y_0}{\sigma_y}\right)^2} e^{-\left(\frac{z-D_p}{\sigma_z}\right)^2}, \tag{3}$$

where α is a constant source term in Pascals, y is across-slip distance, y_0 is the across-slip location of the maximum stress, σ_y is a measure of the spread of stress with across-slip distance z is the depth of the bed, D_p is the depth of the vessel propeller, and σ_z is a measure of the spread of stress with depth. The details of the model calculations are described in Appendix .

Using this model allows us to determine the spatial characteristics of an average

vessel departure wash. The structure of the wash is governed by the spread parameters, σ_y and σ_z. These represent, in a physical sense, how strongly the turbulence advects and diffuses away from the propeller horizontally and vertically. The strength of the wash is governed by the source term α. The wash strength is independent of the wash geometry, and is thus a function of only vessel characteristics. For this model, we will fit α empirically. In reality, α likely depends on the force the vessel exerts on the water as it arrives at or departs the slip. Thus, this model gives insight into the strength of the wash and its across-slip spatial distribution between the two pilings.

This model shows good skill at reproducing the stress profiles at each piling, particularly for smaller depths. It captures the horizontal variability of the stress well, and does well vertically to approximately 9 m depth. Deeper than this, the model under-predicts the stress observed (Figure 11). It should be noted that the stresses observed for depths greater than 9 m come only from the north piling of Slip 1, at the bottom of the cliff face. It is possible that the discrepancy between the modeled and observed stress is a result of the bathymetry at this location; the stress may be enhanced due to self-advection of the turbulence down the cliff face. Additionally, at higher positions in the water column, the model underpredicts the observed stress. This might indicate that the near-surface velocity does not decrease, as a Gaussian model would predict.

This model may be used to predict the expected stress at different horizontal locations on the seabed, for different water depths. It does not depend on local bathymetry, and so it is portable to other Washington State Ferries terminals. Calibrated for other vessels, it could also provide information about scour potential in other ferry and vessel systems. It is important to note that this version of the model, with a constant α, is only valid when

Figure 11: Model results and validation
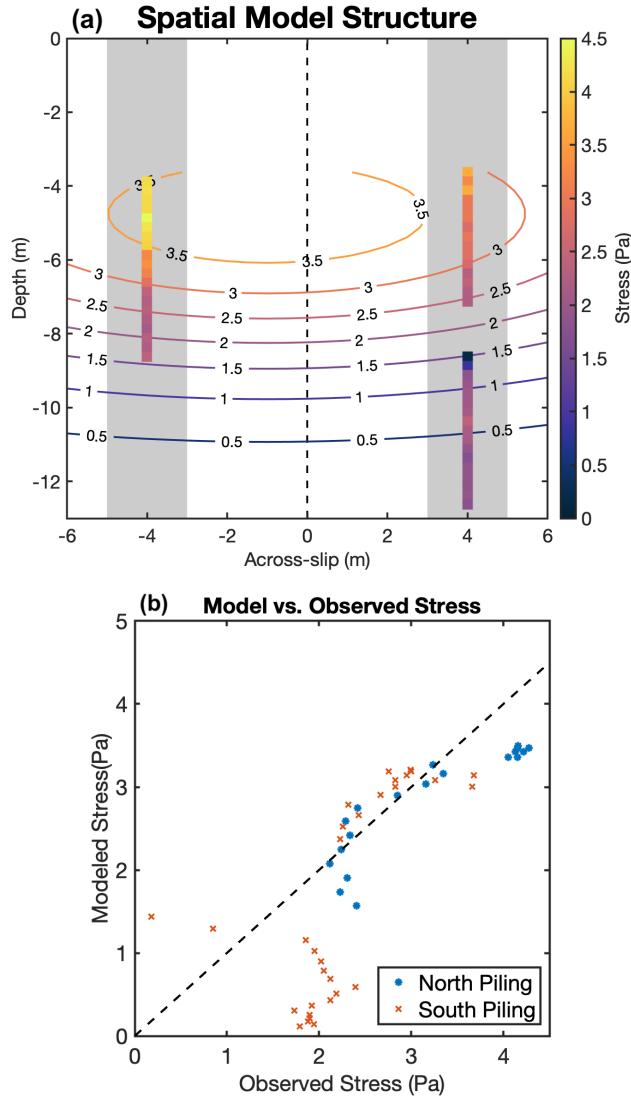
Figure 11: (a) shows the spatial variability of model results as contours of constant stress (in Pa) and the depth profiles of stress at each piling as a colored square (using the same color scale as the contours, shown by the color bar). Model stress contours are not shown above the minimum sensor depth. The grey shaded regions are the approximate locations of the pilings, and the black dashed line is the centerline of the slip. (b) shows the observed vs. modelled stresses at the south and north pilings. The dashed black line shows the 1:1 line.

depth dependence is more important than vessel class dependence. When vessel class dependence dominates, α will need to be changed to account for the influence of the varying mass of the vessel. The observed differences in stress by vessel class were presented in section and Figure 10, which provide preliminary estimates of how much α might change between vessels of differing displacement.

It is important to note that this model predicts bed stress, not scour. Predictions of scour require information about the seabed sediment in addition to the applied stress. Relationships between stress and scour may be developed for this or other sites based on observations of stress and scour taken over longer time periods, or may be adopted from studies of scour in rivers or other coastal settings.

MODEL APPLICATION

Long term analysis

The model developed in section can be applied to a time series of vessel arrival and departure information to assess the stress on the seabed of any vessel arrival or departure, and thus the cumulative stress on the seabed over a period of time. The bed stress during vessel departures can be found using the model, as long as the depth is known at the time of departure. During vessel arrivals, the bed stress can be parameterized as a function of vessel displacement, and can thus be found as long as the displacement of the arriving vessel is known.

We applied the model to 9 years (2010-2019) of vessel arrival and departure logs from the Kingston ferry terminal provided by WSF and publicly available National Oceanic and Atmospheric Administration (NOAA) tide gauge data at Kingston–Appletree Cove. We used the tidally modulated depth of the ADV at the south piling of each slip to predict stress during vessel departures. To predict stress for vessel arrivals, we parameterized stress as proportional to vessel displacement, with a variable constant of proportionality depending on the vessel class as discussed in section . These values are 8×10^{-4} and 6.5×10^{-4} Pa/long ton for Jumbo Mark II class vessels, such as the MV Puyallup, and Jumbo class vessels, such as the MV Walla Walla, respectively. We assumed that for other vessel classes, the average of these values (6.5×10^{-4} Pa/long ton) would be an appropriate scale factor, noting that most arrivals and departures during the period were Jumbo and Jumbo Mark II class vessels. Based on our conversations with WSF representatives, we assumed that the first departure and last arrival of each day were at Slip 2, with all other

vessel arrivals and departures located at Slip 1. We assume a wash duration of 140 seconds, the window length of our calculation of stress from section .

This model application yields a nearly linear cumulative stress over the course of the 9 year period, indicating that for longer time periods, the primary predictive factor of seabed stress is the frequency of vessel arrivals and departures at a given slip (Figure 12a). Thus, Slip 1 experiences more cumulative stress than Slip 2, as expected. On a daily time scale, there is variability in the stress caused by a given arrival or departure, but the linear trend of cumulative stress indicates that this variability can be taken as a constant on longer time scales (greater than one to two weeks). The average value of stress associated with this linear increase is 3.4 Pa, with a slightly smaller average stress on arrivals (3.1 Pa) than departures (3.7 Pa). The stresses predicted by the model are consistent with those we observed, although the constant stress parameterization for arrivals of a given vessel class results in the arrival stresses being considerably more narrow-banded than the departure stresses, which vary with depth (Figure 12b).

Ground line stress

It is important to consider the stress on the ground line when designing a solution to the scour problem at Kingston. If we assume that the wash does not decay significantly away from the propeller in the along-slip direction, as we show in section , we can apply the model at the seabed everywhere along a ground line for vessel departures. We use three ground lines for this analysis: the 2018 survey data for Slip 1 and Slip 2, and a proposed ground line at Slip 1 that fills in the region near the cliff face (Figure 13). The model dictates

Figure 12: Modelled cumulative stress and stress distribution over a 10-year period
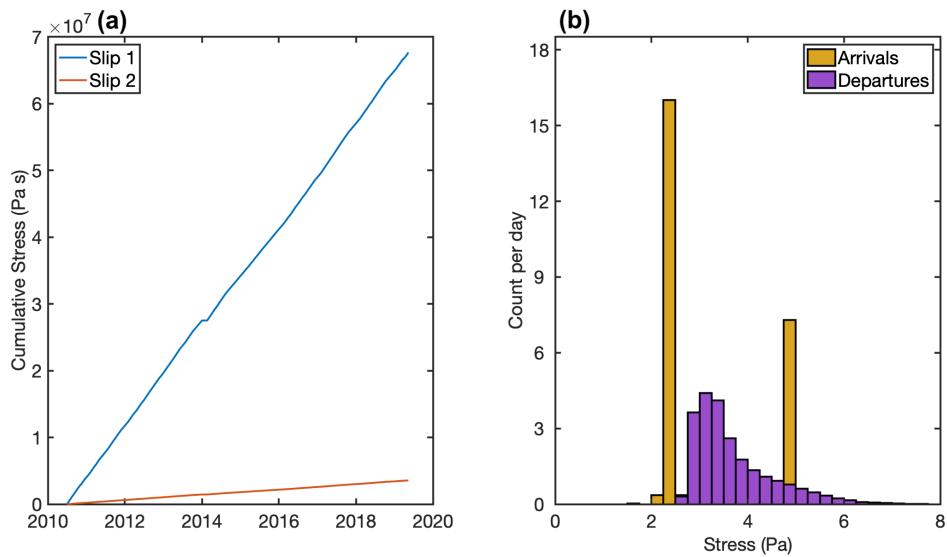
Figure 12: (a) Prediction of cumulative stress for the years 2010-2019 using the model and trends in this report (blue indicates Slip 1, red indicates Slip 2); (b) Histograms of the predicted stress for arrivals and departures, normalized into a daily frequency of each 0.25 Pa stress bin.

that the stress will increase when the bed is closer to the water surface (depth decreases). The model predicts that the fill groundline at Slip 1 will experience higher stresses than the current ground line by a factor of 3, at maximum. This increase must be taken into account when planning the type of sediment to be used in the fill.

The ground line stress is strongly dependent on the specific along-slip bathymetry profile. For example, Slip 1 has smaller stresses everywhere except by the cliff face near the pilings. Therefore, a lower fill line or different fill profile could reduce the stress on the fill. This balance of higher stress at shallower depth needs to be considered as a trade off with a more dissipative, milder slope.

Our results do not directly include the effects of the bathymetry on the wash. In other words, the calculations for the fill profile are made based on the magnitude of the stress at each depth with the current bathymetry. It is reasonable to believe that the stresses may change when the bathymetry is changed. A full hydrodynamic model is necessary to make these predictions properly, but some insight can be gained based on our comparison of Slips 1 and 2. In general, the speed will increase as the depth decreases to conserve the flow rate of the wash. Between Slips 1 and 2 the decrease of average depth by 3.2 m results in an increase in the maximum velocity of 30 cm/s. The proposed groundline represents a reduction in the average depth in the region 10m in front of the piling by 70%. Based on the Slip 1 and Slip 2 comparison one might expect an increase in the average velocity of approximately 60 cm/s. Stress is related to maximum velocity (see Figure 4), so this might result in an increase in stress. It is important to note that the higher maximum velocities at Slip 2 are associated with lower stress. This may be due to a shorter wash duration as the wash propogates by the pilings, as opposed to reflecting off the cliff face at Slip 1.

Figure 13: Ground line depth and stress
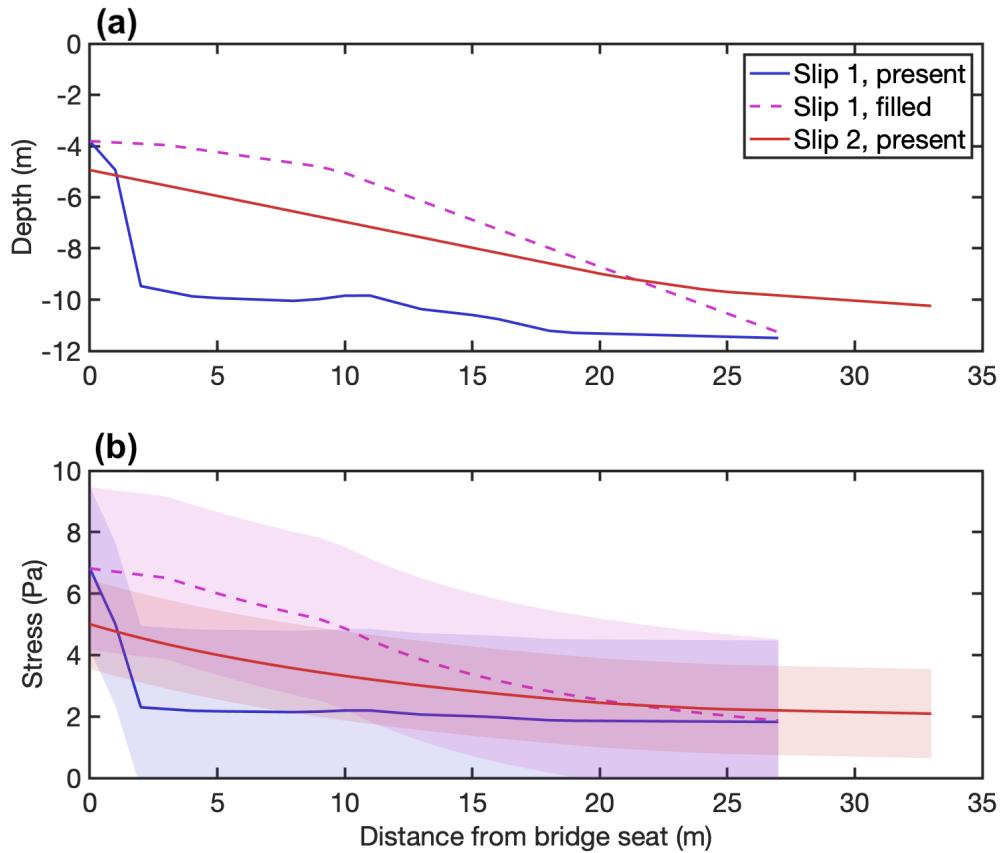
Figure 13: Along-slip profiles of (a) ground line, for Slip 1 (current and proposed) and Slip 2, and (b) stress at the groundline calculated using the model from section . Shaded error bars indicate one half of the standard deviation of stress (mean of the two pilings) observed at each slip.

SUMMARY

Extreme scour at the Kingston ferry terminal is likely caused by ferry arrivals and departures, which lead to high near-bed velocities and stresses at the end of the terminal. Our study uses state-of-the-art velocity measurements to characterize the vessel wake and wash structure and form a predictive model based on the dependencies of near-bed velocity and stress.

During vessel arrivals and departures, maximum near-bed velocities exceed 1 m/s multiple times each day. These maximum velocities vary from slip to slip and piling to piling, indicating that the vessel wake and wash structure is complex and influenced by local bathymetry. The onshore and offshore components of the maximum along-slip velocity is also different between the two slips, as the milder slope of Slip 2 dissipates the wake and wash energy, while the steeper slope of Slip 1 reflects it.

Vessel arrivals and departures cause high bed stresses at the seabed of both slips at the Kingston, WA ferry terminal. These bed stresses are $\sim 100\times$ larger than background stresses due to the turbulent nature of the ferry propeller wash. Furthermore, vessel departures have higher associated bed stresses than vessel arrivals, and vessel departures at lower tidal stages cause higher bed stress than those at higher tidal stages. The higher stress upon vessel departure is likely due to larger accelerations during departure than arrival. Vessel arrivals do not show a depth dependence, but larger vessel displacement is associated with higher bed stress during arrivals. Thus, the largest vessel-influenced bed stresses occur during vessel departures at low water, and the lowest vessel-influenced bed stresses occur during the arrivals of smaller vessels. An empirical model of bed stress during departures

replicates this behavior.

Applying this empirical model to 9 years of vessel activity and tide data yields a nearly linear increase in cumulative stress during this time period, with an average stress of 3.4 Pa. We therefore conclude that for long time scales, vessel frequency is the most important factor in predicting erosion. We also use the model to calculate stress at the ground line of each slip, including a proposed Slip 1 bathymetry. We find that filling in the scour hole and cliff face at Slip 1 will cause the stress on the seabed to increase by a factor of 3 as the depth decreases.

Effective modifications to slip 1 would fill the scour hole and cliff face, with at least the top layer of this fill composed of large (> 5 cm) cobbles. These will be difficult to mobilize. We find that the seabed angle has an impact on whether an incoming wash is reflected or dissipated, and so this fill would ideally be at as close to the angle of Slip 2 as possible in order to more effectively dissipate the wash. We find that vessel frequency is the most important driver of cumulative seabed stress, and so an equal redistribution of vessel arrivals and departures between Slips 1 and 2 would lessen the load on slip 1 .

ACKNOWLEDGEMENTS

REFERENCES

C. Chin, Y. Chiew, S. Y. Lim, and F. H. Lim. Jet scour around vertical pile. *J. Waterway, Port, Coastal, Ocean Eng.*, 122(2):59–67, 1996. doi: https://doi.org/10.1061/(ASCE)0733-950X(1996)122:2(59).

G. A. Hamill, J. A. McGarvey, and P. A. Mackinnon. A method for estimating the bed velocities produced by a ship's propeller wash influenced by a rudder. *Coastal Engineering Proceedings*, 1(26), 1998. URL https://icce-ojs-tamu.tdl.org/icce/index.php/icce/article/view/5867.

J. H. Hong, Y. M. Chiew, and C. N. S. Scour caused by a propeller jet. *Journal of Hydraulic Engineering*, 139(9):1003–1012, 2013. doi: 10.1061/(ASCE)HY.1943-7900.0000746.

P. Julien. *Erosion and Sedimentation*. Cambridge University Press, 2nd edition, 2010. ISBN 978-0-521-83038-6.

A. Shields. *Application of similarity principles and turbulence research to bed-load movement*. PhD thesis, T.U. Delft, 1936. URL http://resolver.tudelft.nl/uuid:a66ea380-ffa3-449b-b59f-38a35b2c6658. Translation of the Ph.D. thesis of A. Shields, 'Anwendung der Aehnlichkeitsmechanik und der Turbulenzforschung auf die Geschiebebewegung'.

R. I. Tan and Y. Yuksel. Seabed scour induced by a propeller jet. *Ocean Engineering*, 160: 132–142, 2018. doi: https://doi.org/10.1016/j.oceaneng.2018.04.076.

L. Wright, J. Chappell, B. Thom, M. Bradshaw, and P. Cowell. Morphodynamics of reflective and dissipative beach and inshore systems: Southeastern australia. *Marine Geology*, 32(1):105 – 140, 1979. ISSN 0025-3227. doi: https://doi.org/10.1016/0025-3227(79)90149-X. URL http://www.sciencedirect.com/science/article/pii/002532277990149X.

Y. Yuksel, S. Kayhan, Y. Celikoglu, and K. Cihan. Open type quay structures under propeller jets. *Coastal Engineering Proceedings*, 1(33), 2012. URL https://icce-ojs-tamu.tdl.org/icce/index.php/icce/article/view/6468.

Y. Yuksel, R. I. Tan, and Y. Celikoglu. Propeller jet flow around a pile structure. *Applied Ocean Research*, 79:160–172, 2018. doi: https://doi.org/10.1016/j.apor.2018.08.001.

APPENDIX: MODEL METHODS

The model in equation 3 is separable into y and z equations, such that a regression can be performed with respect to both across-slip distance and depth in a log-linear sense. We use the ADV data to perform this regression, combining measurements from both slips to produce a profile of stress with depth for the south and north pilings. The spread between the pilings is approximately 8 m, and so the north and south pilings have a position of 4 and -4 m respectively. This coordinate system places the origin in the center of the bridge span at the water surface. We first fit α and σ_z using the z term and the ADV depth and bed stress data. We then take into account this value of α to fit σ_y to the the piling positions and ADV ved stress data, forcing the intercept of the across-slip fit through the origin. The parameters D_p and y_0 are not addressed by the fit, and must be chosen manually. D_p would be equal to the depth of the propeller for a model of stress at the propeller's location, but since the pilings are located shoreward of the propeller, we take D_p as equal to the depth of maximum stress in the south piling stress profile, $D_p = 5$ m. y_0 must be negative (closer to the south piling) because of the higher stresses and correlations with depth at the south pilings, and so we choose a y_0 such that the model fits the calculated stress profiles reasonably well, $y_0 = -1$ m (Figure 11). We further observe that the fitted value of σ_y underpredicts the spread seen between the depth profiles at each piling. In Figure 11, we multiply σ_y by a factor of 2, which compensates for this difference. We thus calculate $\alpha = 4.4$ Pa, $\sigma_y = 13.1$ m, and $\sigma_z = 3.9$ m.